Electronic Supplementary Material (ESI) for Environmental Science: Nano.

Electronic Supplementary Information

Effects of natural organic matter (NOM), metal-to-sulfide ratio and Mn^{2+} on cadmium sulfide nanoparticle growth and colloidal stability

Kevin Hoffmann,[a] Iso Christl,[a] Ralf Kaegi[b] and Ruben Kretzschmar[a*]*

[a] ETH Zürich, Institute of Biogeochemistry and Pollutant Dynamics
CH-8092 Zürich, Switzerland

[b] Eawag, Swiss Federal Institute of Aquatic Science and Technology
CH-8060 Dübendorf, Switzerland

*Corresponding author: ruben.kretzschmar@env.ethz.ch

44 pages, 12 figures, 9 tables

Table of Contents

1. TEM images of CdS suspensions

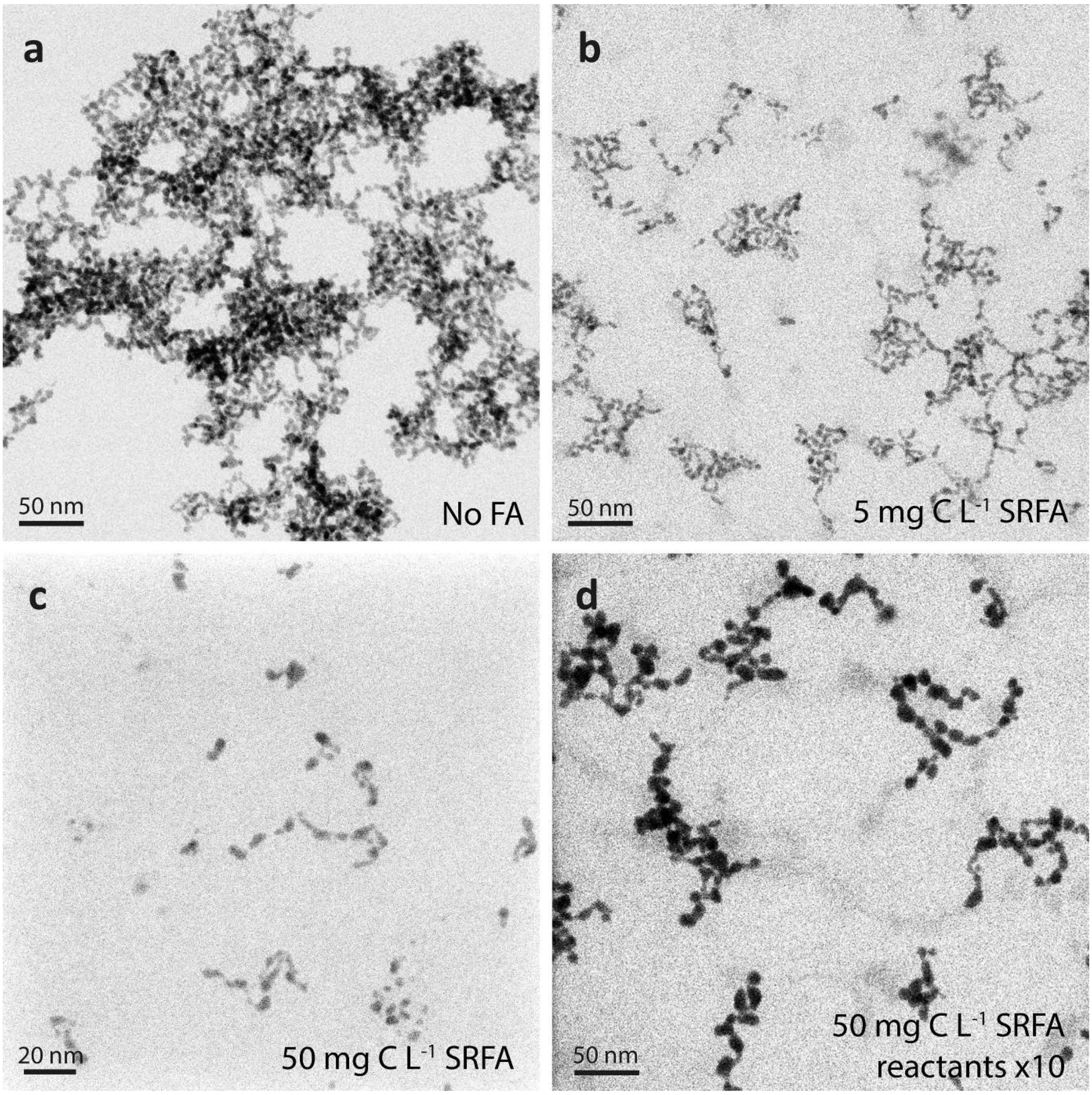

Figure S1: HAADF-TEM images (shown as inverted images) of the CdS suspensions from Fig. 1. TEM images (a-c) present dilute CdS suspensions (50 µmol L^{-1} Cd(II) and 100 µmol L^{-1} S(-II)) in the absence and presence of SRFA (0, 5, 50 mg C L^{-1}) and (d) depicts TEM images of a concentrated CdS suspension (500 µmol L^{-1} Cd(II) and 1000 µmol L^{-1} S(-II)) in the presence of 50 mg C L^{-1} SRFA.

2. Thermodynamic modeling with Visual MINTEQ

Speciation of different reagent mixtures used for the formation of CdS nanoparticles was modelled with Visual MINTEQ 3.1[1] *before* and *after* sulfide addition. Default databases (comp_2008.vdb, thermo.vdb, type6.vdb, Gaussian.vdb) as part of Visual MINTEQ were used. To include Cd complexation on SRFA, the NICA-Donnan model was applied with the generic fulvic acid parameters published by Milne et al. (2003).[2] For activity corrections, we used the Davies equation with the parameter value b = 0.3. Oversaturated solids were allowed to precipitate in each iteration step. Gas equilibria were not included in the calculations. All calculations were performed at 25 °C. To account for reducing conditions in the glovebox, redox potential was fixed at Eh = -100 mV for all calculations. In accordance with the Visual MINTEQ documentation,[1] the output species given in the chemical speciation modeling have the following nomenclature:

- The term “D” generally denotes the concentration of a metal in the so-called Donnan-phase.
- The numbers “6”, “7”, “8” and “9” have no conceptual significance; they are only used by Visual MINTEQ to distinguish different humic components, and they reflect the order in which the components appear on the NICA-Donnan output (with 6 as the starting number).
- (6)Metal+2D(aq): weakly (electrostatically) bound metal to dissolved fulvic acid.
- FA1-metal(aq), FA2-metal(aq): organically complexed metal to dissolved fulvic acid. Sites 1 and 2 refer to carboxylic and phenolic functional groups of the fulvic acid, respectively.

Table S1: Speciation of reagent mixtures (a-e) used for formation of CdS nanoparticles *before* sulfide addition as calculated with Visual MINTEQ 3.1. Reagent mixtures with different SRFA concentrations and absolute concentrations are presented.

---

a) 50 µmol L^{-1} Cd (II), 0 µmol L^{-1} S(-II), 0 mg C L^{-1} SRFA

Input

Species	Na^+ (mol L^{-1})	Cl^- (mol L^{-1})	MOPS (mol L^{-1})	SRFA (mg C L^{-1})	Cd(II) (µmol L^{-1})	pH
Concentration	0.01	0.01	0.001	0	50	7.5

Distribution of components between dissolved and precipitated species (in mol L^{-1})

Component	Total dissolved	% dissolved	Total precipitated	% precipitated
Cd(II)	5.00E-05	100.00	0	0
Cl^-	1.00E-02	100.00	0	0

Dissolved data

Component	% of total concentration	Species
Cd^{2+}	60.6	Cd+2
	1.3	CdCl2(aq)
	0.1	CdOH+
	38.0	CdCl+
MOPS-1	69.7	MOPS-1
	30.3	H-MOPS(aq)

Solids data

Mineral	Saturation index (= log IAP – log Ks)	Minerals precipitated	Equilibrium amount (mol L^{-1})
CdOHCl(s)	-2.783	none	0
$Cd(OH)_2(s)$	-3.342		
$CdCl_2(s)$	-8.135		

b) 50 µmol L^{-1} Cd (II), 0 µmol L^{-1} S(-II), 5 mg C L^{-1} SRFA

Input

Species	Na^+ (mol L^{-1})	Cl^- (mol L^{-1})	MOPS (mol L^{-1})	SRFA (mg C L^{-1})	Cd(II) (µmol L^{-1})	pH
Concentration	0.01	0.01	0.001	5	50	7.5

Distribution of components between dissolved and precipitated species (in mol L^{-1})

Component	**Total dissolved**	**% dissolved**	**Dissolved inorganic**	**Bound to DOM**	**% bound to DOM**	**Total precipitated**	**% precipitated**
Cd(II)	5.00E-05	100.00	3.94E-05	1.06E-05	21.3	0	0
Cl^-	1.00E-02	100.00	1.00E-02	0	0	0	0

Dissolved data

Component	**% of total concentration**	**Species**
Cd^{2+}	47.7	Cd+2
	0.1	FA2-Cd(6)(aq)
	0.1	(6)CdCl+D(aq)
	0.1	CdOH+
	30.0	CdCl+
	1.0	CdCl2
	8.2	(6)Cd+2D(aq)
	12.9	FA1-Cd(6)(aq)
HFA1-(6)(aq)	84.8	HFA1-(6)(aq)
	1.9	FA1-H(6)(aq)
	13.3	FA1-Cd(6)(aq)
HFA2-(6)(aq)	2.7	HFA2-(6)(aq)
	97.1	FA2-H(6)(aq)
	0.2	FA2-Cd(6)(aq)
MOPS-1	69.7	MOPS-1
	30.3	H-MOPS (aq)

Solids data

Mineral	**Saturation index (= log IAP – log Ks)**	**Minerals precipitated**	**Equilibrium amount (mol L^{-1})**
CdOHCl(s)	-2.887	none	0
$Cd(OH)_2(s)$	-3.446		
$CdCl_2(s)$	-8.238		

c) 50 µmol L^{-1} Cd (II), 0 µmol L^{-1} S(-II), 50 mg C L^{-1} SRFA

Input

Species	Na^{+} (mol L^{-1})	Cl^{-} (mol L^{-1})	MOPS (mol L^{-1})	SRFA (mg C L^{-1})	Cd(II) (µmol L^{-1})	pH
Concentration	0.01	0.01	0.001	50	50	7.5

Distribution of components between dissolved and precipitated species (in mol L^{-1})

Component	**Total dissolved**	**% dissolved**	**Dissolved inorganic**	**Bound to DOM**	**% bound to DOM**	**Total precipitated**	**% precipitated**
Cd(II)	5.00E-05	100.00	4.53E-06	4.55E-05	90.9	0	0
Cl^{-}	1.00E-02	100.00	1.00E-02	0	0	0	0

Dissolved data

Component	**% of total concentration**	**Species**
Cd^{2+}	5.5	Cd+2
	0.2	FA2-Cd(6)(aq)
	0.1	(6)CdCl+D(aq)
	0.01	CdOH+
	3.5	CdCl+
	0.1	CdCl2
	20.6	(6)Cd+2D(aq)
	70.0	FA1-Cd(6)(aq)
HFA1-(6)(aq)	89.4	HFA1-(6)(aq)
	3.4	FA1-H(6)(aq)
	7.2	FA1-Cd(6)(aq)
HFA2-(6)(aq)	2.2	HFA2-(6)(aq)
	97.7	FA2-H(6)(aq)
	0.1	FA2-Cd(6)(aq)
MOPS-1	69.7	MOPS-1
	30.3	H-MOPS (aq)

Solids data

Mineral	**Saturation index (= log IAP – log Ks)**	**Minerals precipitated**	**Equilibrium amount (mol L^{-1})**
CdOHCl(s)	-3.825	none	0
Cd(OH)$_2$(s)	-4.385		
CdCl$_2$(s)	-9.176		

d) 500 µmol L^{-1} Cd (II), 0 µmol L^{-1} S(-II), 0 mg C L^{-1} SRFA

Input

Species	Na^+ (mol L^{-1})	Cl^- (mol L^{-1})	MOPS (mol L^{-1})	SRFA (mg C L^{-1})	Cd(II) (µmol L^{-1})	pH
Concentration	0.01	0.01	0.01	0	500	7.5

Distribution of components between dissolved and precipitated species (in mol L^{-1})

Component	Total dissolved	% dissolved	Total precipitated	% precipitated
Cd(II)	5.00E-04	100.00	0	0
Cl^-	1.00E-02	100.00	0	0

Dissolved data

Component	% of total concentration	Species
Cd^{2+}	61.0	Cd+2
	1.2	CdCl2(aq)
	0.1	CdOH+
	37.6	CdCl+
MOPS-1	69.7	MOPS-1
	30.3	H-MOPS(aq)

Solids data

Mineral	Saturation index (= log IAP – log Ks)	Minerals precipitated	Equilibrium amount (mol L^{-1})
CdOHCl(s)	-1.788	none	0
$Cd(OH)_2$(s)	-2.339		
$CdCl_2$(s)	-7.147		

e) 500 µmol L^{-1} Cd (II), 0 µmol L^{-1} S(-II), 50 mg C L^{-1} SRFA

Input

Species	Na^{+} (mol L^{-1})	Cl^{-} (mol L^{-1})	MOPS (mol L^{-1})	SRFA (mg C L^{-1})	Cd(II) (µmol L^{-1})	pH
Concentration	0.01	0.01	0.01	50	500	7.5

Distribution of components between dissolved and precipitated species (in mol L^{-1})

Component	Total dissolved	% dissolved	Dissolved inorganic	Bound to DOM	% bound to DOM	Total precipitated	% precipitated
Cd(II)	5.00E-04	100.00	3.23E-04	1.77E-04	35.4	0	0
Cl^{-}	1.00E-02	100.00	1.00E-02	0	0	0	0

Dissolved data

Component	% of total concentration	Species
Cd^{2+}	39.3	Cd+2
	0.2	FA2-Cd(6)(aq)
	0.3	(6)CdCl+D(aq)
	0.1	CdOH+
	24.4	CdCl+
	0.8	CdCl2
	17.6	(6)Cd+2D(aq)
	17.3	FA1-Cd(6)(aq)
HFA1-(6)(aq)	81.1	HFA1-(6)(aq)
	1.0	FA1-H(6)(aq)
	17.9	FA1-Cd(6)(aq)
HFA2-(6)(aq)	4.0	HFA2-(6)(aq)
	95.5	FA2-H(6)(aq)
	0.5	FA2-Cd(6)(aq)
MOPS-1	69.7	MOPS-1
	30.3	H-MOPS (aq)

Solids data

Mineral	Saturation index (= log IAP – log Ks)	Minerals precipitated	Equilibrium amount (mol L^{-1})
CdOHCl(s)	-1.976	none	0
$Cd(OH)_2(s)$	-2.530		
$CdCl_2(s)$	-7.332		

Table S2: Speciation of final CdS suspensions (*after* sulfide addition) as calculated with Visual MINTEQ 3.1. Suspensions with different SRFA concentrations and absolute concentrations are presented (a-e).

a) 50 µmol L^{-1} Cd (II), 100 µmol L^{-1} S(-II), 0 mg C L^{-1} SRFA

Input

Species	Na^+ (mol L^{-1})	Cl^- (mol L^{-1})	MOPS (mol L^{-1})	SRFA (mg C L^{-1})	Cd(II) (µmol L^{-1})	S(-II) (µmol L^{-1})	pH
Concentration	0.01	0.01	0.001	0	50	100	7.5

Distribution of components between dissolved and precipitated species (in mol L^{-1})

Component	Total dissolved	% dissolved	Total precipitated	% precipitated
Cd(II)	0	0	5.00E-05	100.00
HS^-	7.84E-07	0.784	9.92E-05	99.22

Solids data

Mineral	Saturation index (= log IAP – log Ks)	Minerals precipitated	Equilibrium amount (mol L^{-1})
Greenockite	0	Greenockite	5.00E-05
Sulfur(s)	0	Sulfur(s)	4.92E-05
CdOHCl(s)	-13.34		
$Cd(OH)_2$(s)	-13.90		
$CdCl_2$(s)	-18.69		

b) 50 µmol L^{-1} Cd (II), 100 µmol L^{-1} S(-II), 5 mg C L^{-1} SRFA

Input

Species	Na^+ (mol L^{-1})	Cl^- (mol L^{-1})	MOPS (mol L^{-1})	SRFA (mg C L^{-1})	Cd(II) (µmol L^{-1})	S(-II) (µmol L^{-1})	pH
Concentration	0.01	0.01	0.001	5	50	100	7.5

Distribution of components between dissolved and precipitated species (in mol L^{-1})

Component	Total dissolved	% dissolved	Total precipitated	% precipitated
Cd(II)	0	0	5.00E-05	100.00
HS^-	7.84E-07	0.784	9.92E-05	99.22

Solids data

Mineral	Saturation index (= log IAP – log Ks)	Minerals precipitated	Equilibrium amount (mol L^{-1})
Greenockite	0	Greenockite	5.00E-05
Sulfur(s)	0	Sulfur(s)	4.92E-05
CdOHCl(s)	-13.34		
$Cd(OH)_2$(s)	-13.90		
$CdCl_2$(s)	-18.69		

c) 50 µmol L^{-1} Cd (II), 100 µmol L^{-1} S(-II), 50 mg C L^{-1} SRFA

Input

Species	Na^+ (mol L^{-1})	Cl^- (mol L^{-1})	MOPS (mol L^{-1})	SRFA (mg C L^{-1})	Cd(II) (µmol L^{-1})	S(-II) (µmol L^{-1})	pH
Concentration	0.01	0.01	0.001	50	50	100	7.5

Distribution of components between dissolved and precipitated species (in mol L^{-1})

Component	**Total dissolved**	**% dissolved**	**Total precipitated**	**% precipitated**
Cd(II)	0	0	5.00E-05	100.00
HS^-	7.84E-07	0.784	9.92E-05	99.22

Solids data

Mineral	**Saturation index (= log IAP – log Ks)**	**Minerals precipitated**	**Equilibrium amount (mol L^{-1})**
Greenockite	0	Greenockite	5.00E-05
Sulfur(s)	0	Sulfur(s)	4.92E-05
CdOHCl(s)	-13.34		
$Cd(OH)_2$(s)	-13.90		
$CdCl_2$(s)	-18.69		

d) 500 µmol L^{-1} Cd (II), 1000 µmol L^{-1} S(-II), 0 mg C L^{-1} SRFA

Input

Species	Na^+ (mol L^{-1})	Cl^- (mol L^{-1})	MOPS (mol L^{-1})	SRFA (mg C L^{-1})	Cd(II) (µmol L^{-1})	S(-II) (µmol L^{-1})	pH
Concentration	0.01	0.01	0.01	0	500	1000	7.5

Distribution of components between dissolved and precipitated species (in mol L^{-1})

Component	Total dissolved	% dissolved	Total precipitated	% precipitated
Cd(II)	0	0	5.00E-04	100.00
HS^-	7.84E-07	0.784	9.92E-04	99.22

Solids data

Mineral	Saturation index (= log IAP – log Ks)	Minerals precipitated	Equilibrium amount (mol L^{-1})
Greenockite	0	Greenockite	5.00E-04
Sulfur(s)	0	Sulfur(s)	4.99E-04
CdOHCl(s)	-13.34		
$Cd(OH)_2(s)$	-13.90		
$CdCl_2(s)$	-18.69		

e) 500 µmol L^{-1} Cd (II), 1000 µmol L^{-1} S(-II), 50 mg C L^{-1} SRFA

Input

Species	Na^+ (mol L^{-1})	Cl^- (mol L^{-1})	MOPS (mol L^{-1})	SRFA (mg C L^{-1})	Cd(II) (µmol L^{-1})	S(-II) (µmol L^{-1})	pH
Concentration	0.01	0.01	0.01	50	500	1000	7.5

Distribution of components between dissolved and precipitated species (in mol L^{-1})

Component	Total dissolved	% dissolved	Total precipitated	% precipitated
Cd(II)	0	0	5.00E-04	100.00
HS^-	7.84E-07	0.784	9.92E-04	99.22

Solids data

Mineral	Saturation index (= log IAP – log Ks)	Minerals precipitated	Equilibrium amount (mol L^{-1})
Greenockite	0	Greenockite	5.00E-04
Sulfur(s)	0	Sulfur(s)	4.99E-04
CdOHCl(s)	-13.34		
$Cd(OH)_2$(s)	-13.90		
$CdCl_2$(s)	-18.69		

3. Hydrodynamic diameters and zeta potential of CdS suspensions in the absence and presence of SRFA

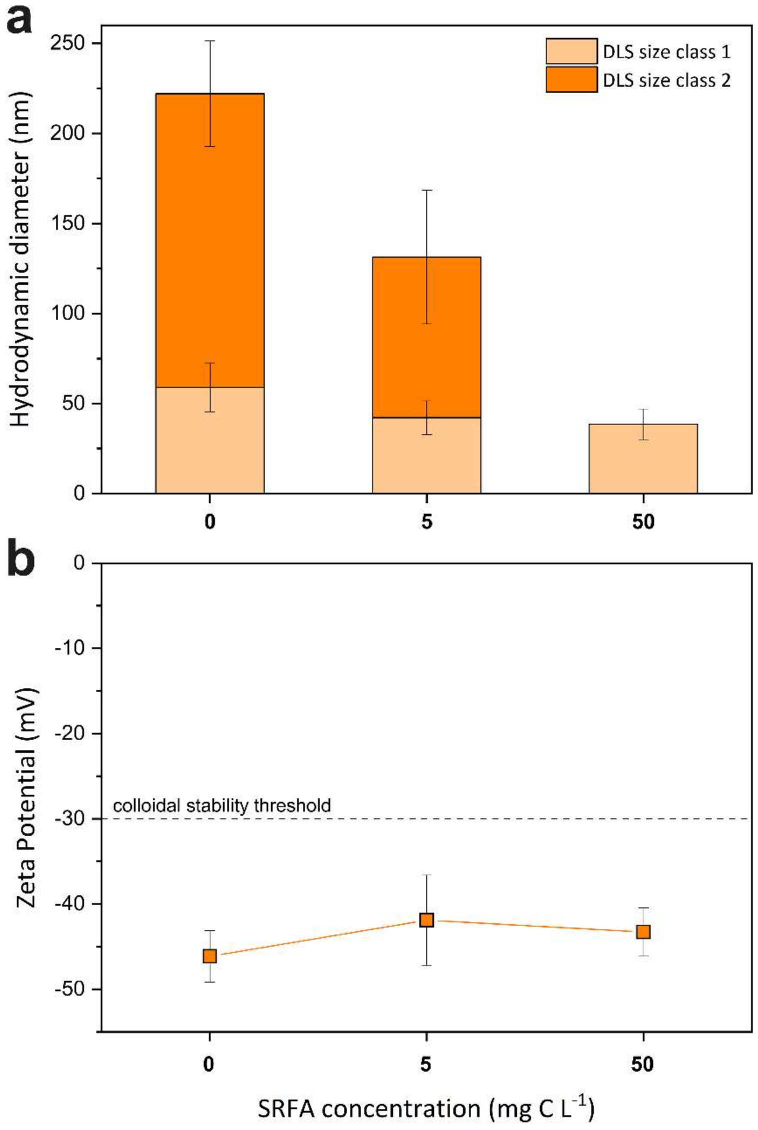

Figure S2: Influence of fulvic acid concentration on median hydrodynamic diameters $\tilde{d}_h$ (a) and zeta potentials (b) of dilute CdS suspensions (50 µmol L^{-1} Cd(II) and 100 µmol L^{-1} S(-II)) at pH 7.5 and 10 mmol L^{-1} NaCl electrolyte after 24h equilibration time. Due to bimodal size distributions of the NPs, two size classes were considered for size evaluation using the multi narrow mode algorithm in the DLS software. All values were compiled from at least two sample replicates (n = 2–5). The dashed line in (b) at -30 mV indicates the electrostatic colloidal stability threshold.

4. TEM primary particle size and aggregate size distributions and TEM images of CdS suspensions with 1:1 and 2:1 metal-to-sulfide ratio

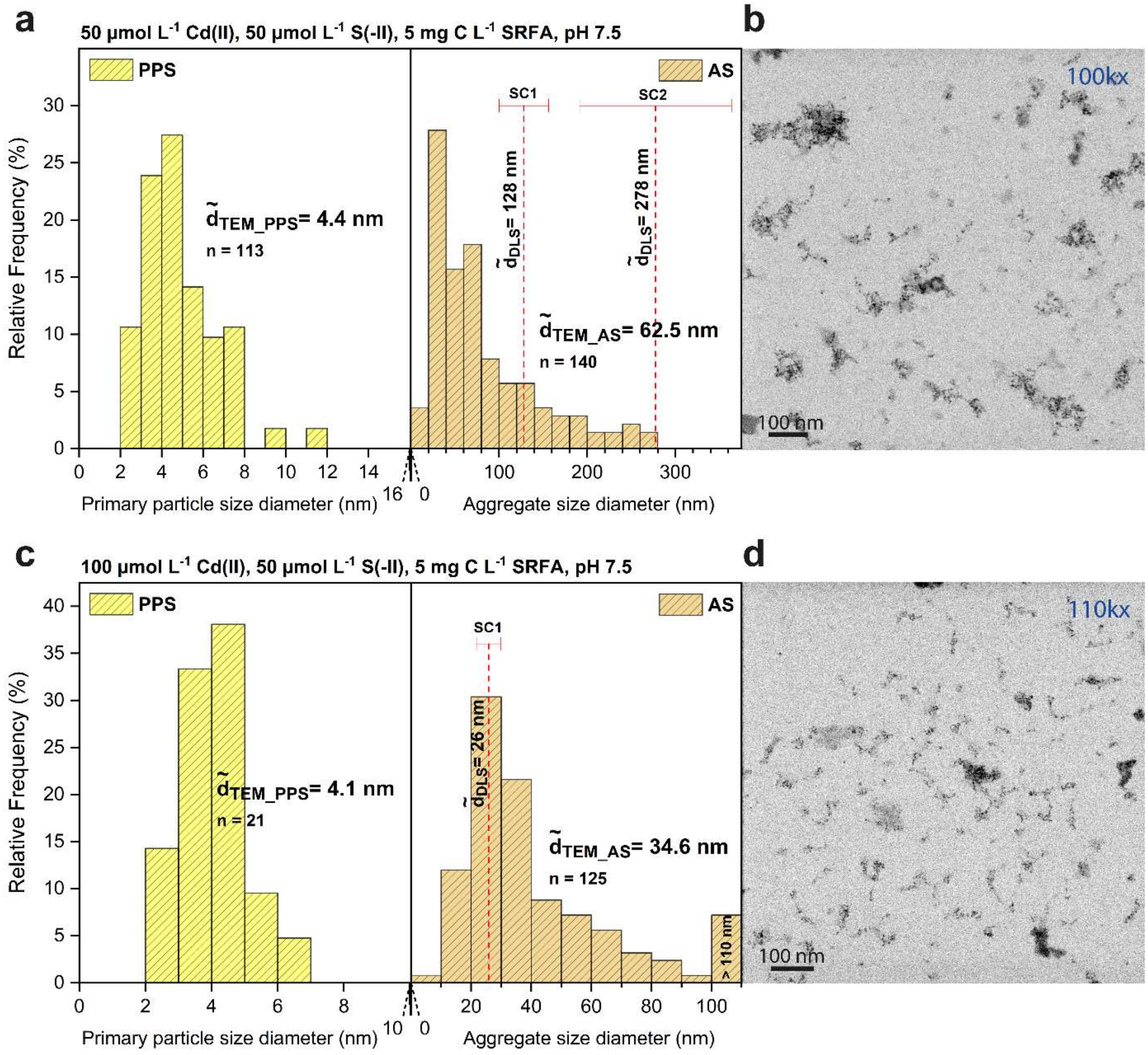

Figure S3: TEM primary particle size (PPS) and aggregate size (AS) distributions of CdS suspension with 1:1 (a and b) and 2:1 (c and d) ratio of reactants with median TEM diameters ($\tilde{d}_{\text{TEM}}$) and median hydrodynamic diameters ($\tilde{d}_{\text{DLS}}$). Median hydrodynamic diameters are shown in two considered size classes (SC1: smaller size class, SC2: larger size class). Representative HAADF-TEM images (shown as inverted images) of the corresponding CdS nanoparticles are depicted on the right side next to the particle size distributions. Background solutions consisted of 10 mmol L^{-1} NaCl at pH 7.5 (1 mmol L^{-1} MOPS buffer).

5. Comparison of TEM and DLS sizes, and zeta potentials with significance tests

Table S3: CdS batch overview showing median TEM and hydrodynamic diameters (with standard deviation) as well as zeta potentials (with standard deviation) of selected suspensions including tests on statistical significance among variants. Letters behind the numbers designate significant differences among sample variants ($p<0.05$; Mann-Whitney-Test).

Sample	Median diameter (nm)				Zeta potential (mV)
	TEM		DLS		
Effect – NOM concentration	**PPS**	**AS**	**Size class 1**	**Size class 2**	
50 µmol L^{-1} Cd(II), 100 µmol L^{-1} S(-II), No SRFA	7.4a	167.0a	58.9a±13.5	222.0a±29.3	-46.2a±3.0
50 µmol L^{-1} Cd(II), 100 µmol L^{-1} S(-II), 5 mg C L^{-1} SRFA	6.9b	42.7b	42.1b±9.3	131.3b±37.2	-41.9ab±5.3
50 µmol L^{-1} Cd(II), 100 µmol L^{-1} S(-II), 50 mg C L^{-1} SRFA	5.1c	18.5c	38.5b±8.5	—	-43.3b±2.8
Effect – Reactant concentrations					
50 µmol L^{-1} Cd(II), 100 µmol L^{-1} S(-II), 5 mg C L^{-1} SRFA	6.9a	42.7a	42.1a±9.3	131.3a±37.2	-41.9a±5.3
500 µmol L^{-1} Cd(II), 1000 µmol L^{-1} S(-II), 50 mg C L^{-1} SRFA	6.0a	44.1a	32.4b±2.2	116.5a±6.7	-46.5b±0.8
Effect – Metal-to-sulfide ratio					
50 µmol L^{-1} Cd(II), 100 µmol L^{-1} S(-II), 5 mg C L^{-1} SRFA	6.9a	42.7ab	42.1a±9.3	131.3a±37.2	-41.9a±5.3
50 µmol L^{-1} Cd(II), 50 µmol L^{-1} S(-II), 5 mg C L^{-1} SRFA	4.4b	62.5a	128.1b±28.0	277.5b±86.3	-44.6a±2.6
100 µmol L^{-1} Cd(II), 50 µmol L^{-1} S(-II), 5 mg C L^{-1} SRFA	4.1b	34.6b	25.9c±4.1	—	-35.8b±1.9

6. Energy dispersive X-ray (EDX) spectra of CdS nanoparticles recorded in the TEM

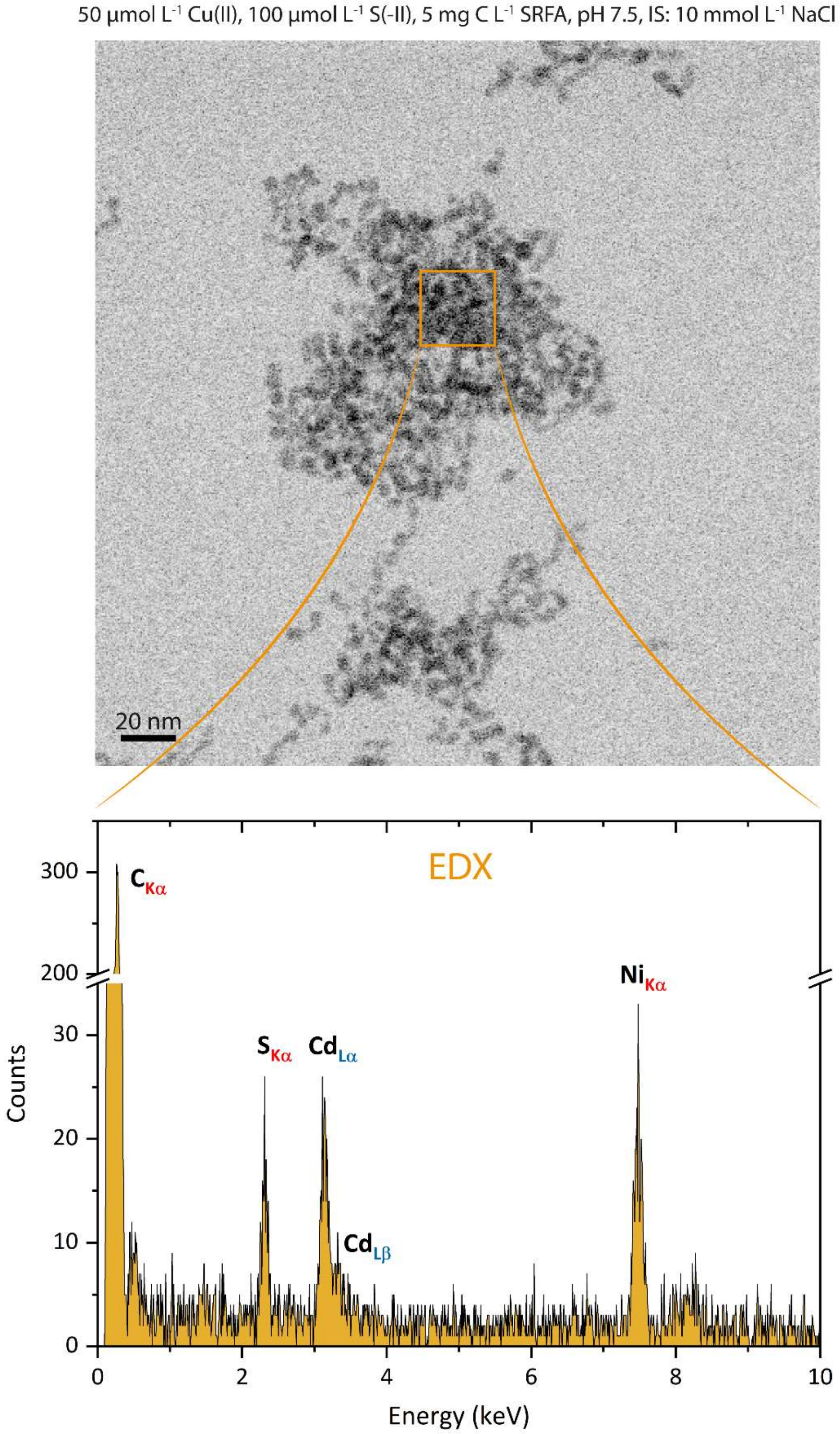

Figure S4: EDX spectrum and corresponding HAADF-TEM image (shown as inverted image) of a typical CdS aggregate (marked aggregate in the inset image). Peaks of Kα lines of the elements of interest are labelled. The $Ni_{K\alpha}$ peak at 7.48 keV is due to the used Ni grid (TEM sample holder).

7. HR-TEM images and calculated selected area electron diffraction (SAED) of CdS nanoparticles

<u>Composition:</u> 50 µM Cd(II), 100 µM S(-II), 5 mg C/L FA, pH 7.5, IS: 10 mM NaCl

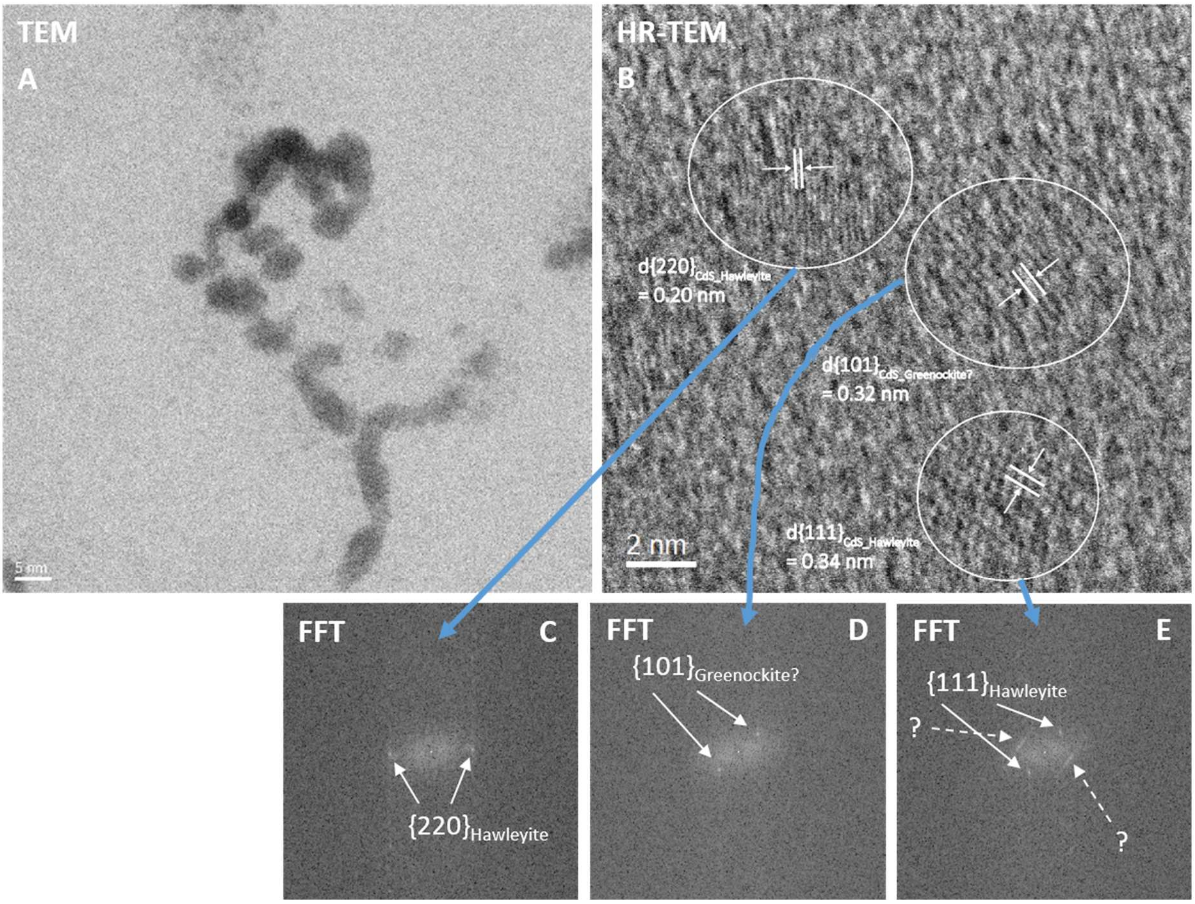

Figure S5: (High-resolution) TEM images (A shown as inverted image and B) and the calculated selected area diffraction pattern (SAED) of CdS (C, D, E). Despite the poorly crystalline character of the particles, crystal lattice planes of hawleyite and greenockite were identified.

8. Solid digestion of CdS-Mn solids

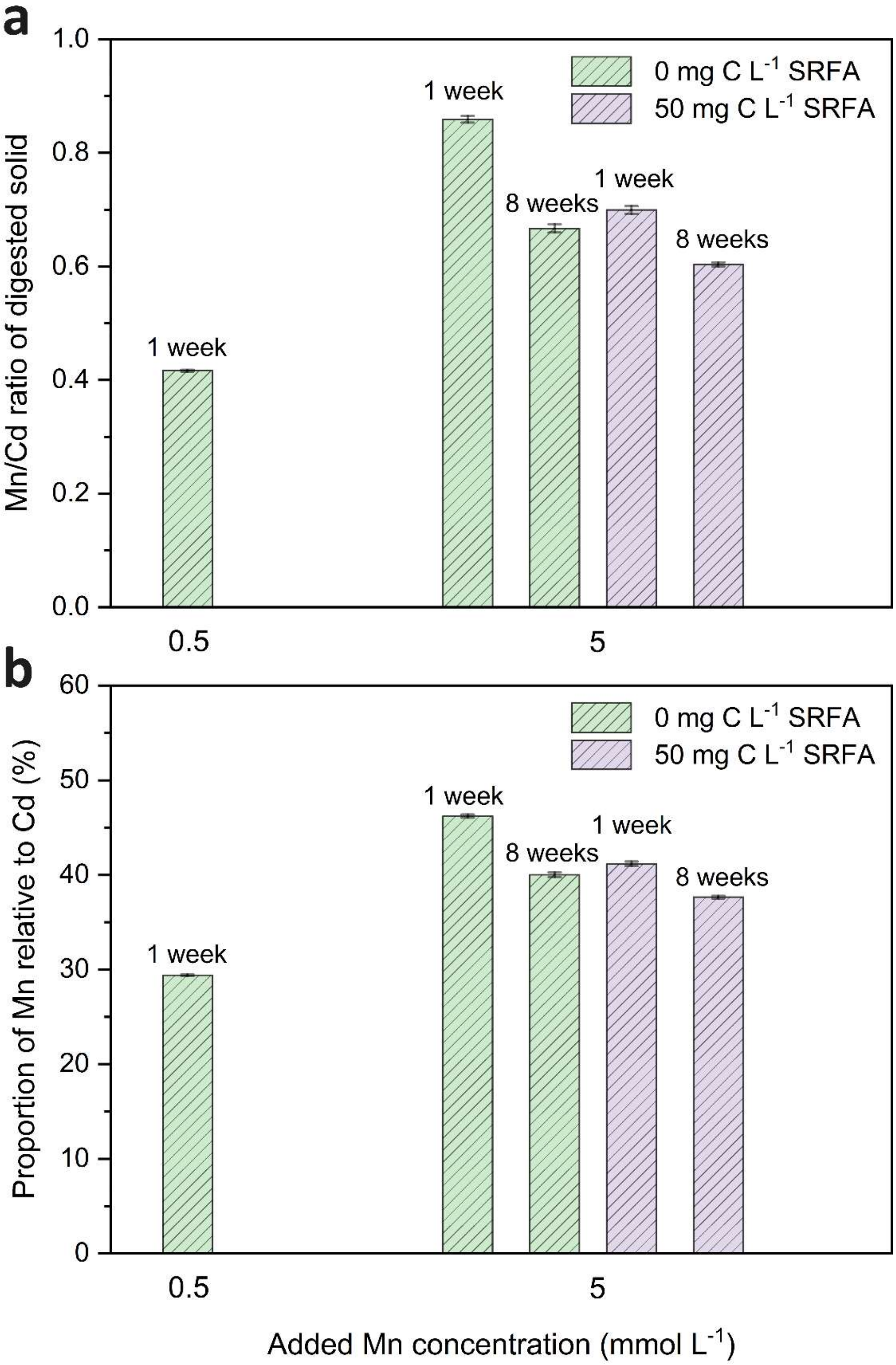

Figure S6: Panel (a) shows the Mn/Cd ratio of a few selected digested CdS solid samples that were incubated at two different Mn^{2+} concentrations (0.5, 5 mmol L^{-1} Mn^{2+}) added to the reacting suspension for 1 and 8 weeks in the absence and presence of SRFA. Panel (b) illustrates the corresponding proportion of Mn in % (relative to the total Cd within the $Cd_xMn_{1-x}S$ solid) that is associated (Mn_{as} = (Mn/(Cd+Mn)) x 100) with the CdS (either adsorbed to the CdS surface, incorporated into crystal structure or coprecipitated with CdS).

9. Rietveld fitting results and Mn substitution inferred by XRD unit cell dimension comparison

Table S4: Rietveld fit results of various concentrated CdS suspensions (500 µmol L^{-1} Cd(II) and 1000 µmol L^{-1} S(-II)) in the absence and presence of Mn^{2+} and SRFA after aging for different time spans. As reference for cell parameters, the ICSD values for greenockite and hawleyite are given. Besides the change in cell parameters of these phases, fitted phase contributions are shown together with respective goodness of fit (GOF = R_{wp}/R_{exp}) values. Additionally, derived Mn substitution from consulting the study results of Rodic et al. (1996)[3] are presented. For comparable reasons, Mn (molar %, relative to total Cd) found in digested $Cd_{1-x}Mn_xS$ solid of this study are given.

No.	Sample	Greenockite			Hawleyite						
		a cell para-meter	c cell para-meter	Phase contri-bution (%)	a cell para-meter	Phase contri-bution (%)	R_{wp}	R_{exp}	Good-ness of fit (GOF)	Mn substitution (%) derived from correlation with (*a*) or (*c*) cell parameter from Rodic et al. (1996)	Mn (molar %) relative to total Cd (=Mn_{tot}) found in digested $Cd_{1-x}Mn_xS$ solid (n=3)
x	ICSD ref. (31074: greenockite & 31075: hawleyite)	4.135	6.749	–	5.818	–	–	–	–	–	–
1	CdS pure – 24 h	4.123	6.732	17	5.823	83	6.43	5.51	1.17	–	–
2	CdS + 50 mg C L^{-1} SRFA – 24 h	4.124	6.729	17	5.822	83	7.43	4.99	1.49	–	–
3	CdS pure – 8 w	4.130	6.832	33	5.834	67	7.26	4.84	1.50	–	–
4	CdS + 0.5 mmol L^{-1} Mn – 1w	4.102	6.682	21	5.784	79	6.64	3.55	1.87	11.5(*c*) – 20.7(*a*)	29.4 ± 0.1
5	CdS + 0.5 mmol L^{-1} Mn – 8w	4.092	6.661	23	5.765	77	5.75	3.79	1.52	19.3(*c*) – 26.9(*a*)	–
6	CdS + 5 mmol L^{-1} Mn – 8w	4.076	6.658	20	5.765	80	6.33	3.77	1.68	20.4(*c*) – 37.5(*a*)	40.0 ± 0.3
7	CdS + 5 mmol L^{-1} Mn + 50 mg C L^{-1} SRFA – 1w	4.124	6.652	21	5.757	79	4.64	3.72	1.25	5.6(*a*) – 22.8(*c*)	41.2 ± 0.2
8	CdS + 5 mmol L^{-1} Mn + 50 mg C L^{-1} SRFA – 8w	4.113	6.641	16	5.766	84	4.35	4.35	1.00	13.1(*a*) – 27.1(*c*)	37.6 ± 0.1

10. XRD diffractograms of CdS and $Cd_{1-x}Mn_xS$ solids

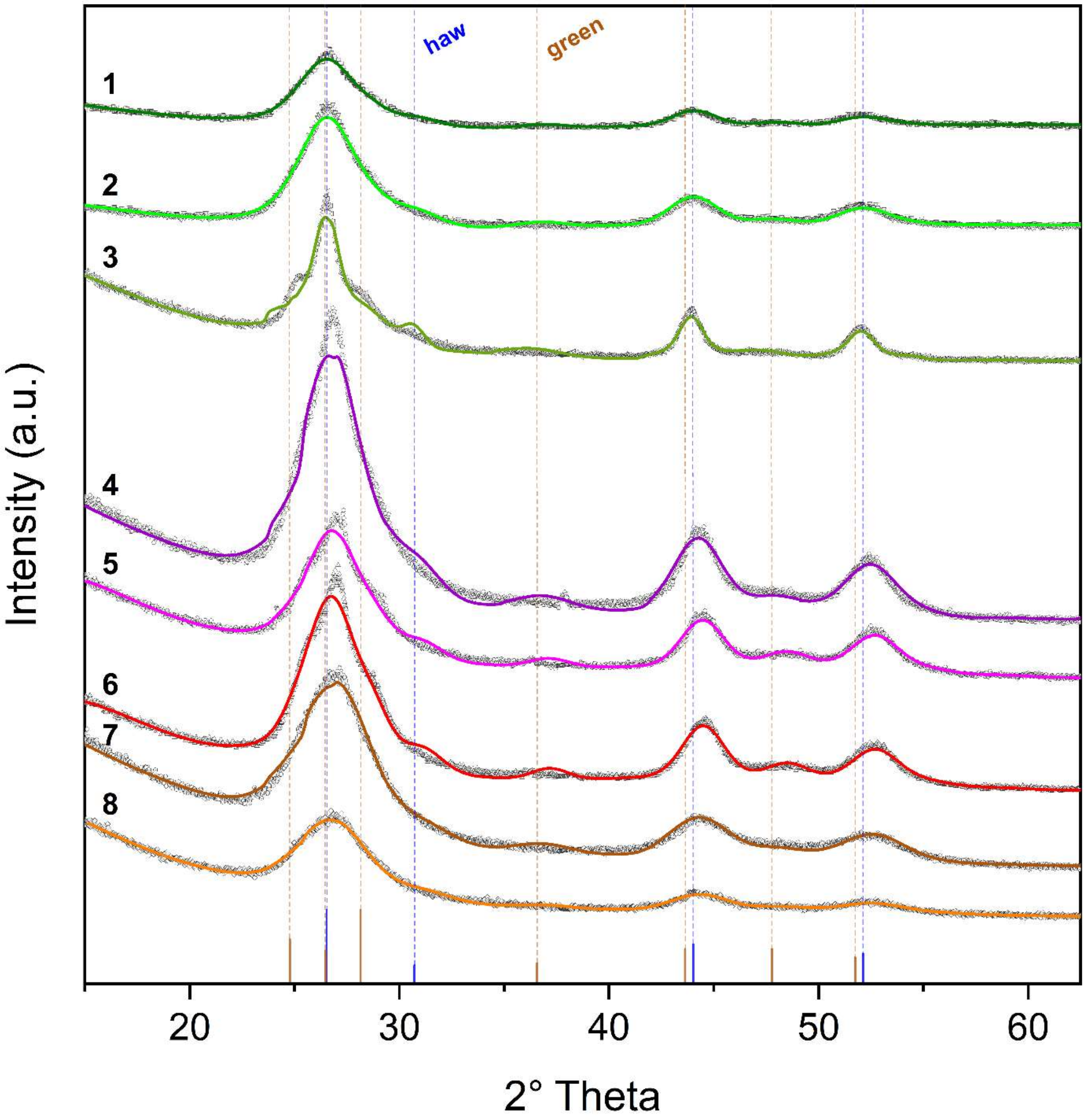

Figure S7: Recorded X-ray diffractograms of CdS (concentrated suspensions at 1:2 metal-to-sulfide ratio: 500 µmol L^{-1} Cd(II) and 1000 µmol L^{-1} S(-II)) in the absence or presence of 50 mg C L^{-1} SRFA and different Mn^{2+} concentrations (0.5 and 5 mmol L^{-1}) shown as gray symbols and corresponding quantitative phase analysis (QPA) using Rietveld fits (colored lines). The bottom part illustrates the major reflections (with their relative intensities) of the CdS phases hawleyite and greenockite. Dashed lines originating from these reflections show the peak matching with the recorded diffractograms. For the sake of clarity, numbers were assigned to the samples. Corresponding sample composition, phase contributions and GOF can be withdrawn from Table S4.

11. Calculations on Mn fractions based on solid digestion data and data inferred from XRD unit cell parameters

In an attempt to quantify respective Mn fractions in the samples, we used Mn/Cd ratios determined from solid digestion data (Fig. S6) and the amount of Mn that was potentially incorporated into the CdS crystal structure (inferred from consulting the study results of Rodic et al. (1996),[3] Fig. 4 and Tab. S4). From a mechanistic point of view, Mn could be present in the following fractions:

- Mn_{inc}: Mn incorporated into the crystal structure of CdS (substituting Cd ions in the crystal lattice)
- Mn_{ads}: Mn adsorbed onto the CdS particle surface
- Mn_{SRFA}: Mn complexed by SRFA functional groups, either a) with SRFA adsorbed onto the CdS surface, or b) Mn complexed by SRFA and flocculated / co-precipitated as a second phase besides colloidal CdS
- Mn_{dis}: free aqueous Mn species in the suspension

From the solid digestion data, we can approximate the total Mn (Mn_{tot}) amount within the solid samples. From the XRD unit cell parameter comparison, we obtain an approximate for the incorporated Mn fraction (Mn_{inc}). For the samples formed in the absence of SRFA, the residual fraction of Mn in Tab. S5 is equal to the adsorbed Mn fraction. In the study of Rodic et al. (1996)[3] that was used for comparison, unit cell parameter changes are only tracked for CdS in the presence of Mn^{2+}, not containing any DOM. Therefore, results calculated for samples containing SRFA should be interpreted with caution.

Table S5: Total Mn (% Mn_{tot}, relative to total Cd) found in digested $Cd_{1-x}Mn_xS$ solid of this study are given together with the derived Mn substitution from consulting the study results of Rodic et al. (1996)[3] and calculated residual Mn fractions.

No.	Sample	Mn total (% Mn_{tot})	Mn incorporated (% Mn_{inc})	Mn adsorbed or Mn residual (% Mn_{ads} or Mn_{res})	Share of Mn_{ads} or Mn_{res} in Mn_{tot} (%)
4	CdS + 0.5 mmol L^{-1} Mn – 1w	29.4 ± 0.1	11.5(*c*) – 20.7(*a*)	8.7 (*a*) – 17.9 (*c*)	29.6 (*a*) – 60.9 (*c*)
6	CdS + 5 mmol L^{-1} Mn – 8w	40.0 ± 0.3	20.4(*c*) – 37.5(*a*)	2.5 (*a*) – 19.6 (*c*)	6.3 (*a*) – 49.0 (*c*)
7	CdS + 5 mmol L^{-1} Mn + 50 mg C L^{-1} SRFA – 1w	41.2 ± 0.2	5.6(*a*) – 22.8(*c*)	18.4 (*c*) – 35.6 (*a*)	44.7 (*c*) – 86.4 (*a*)
8	CdS + 5 mmol L^{-1} Mn + 50 mg C L^{-1} SRFA – 8w	37.6 ± 0.1	13.1(*a*) – 27.1(*c*)	10.5 (*c*) – 24.5 (*a*)	27.9 (*c*) – 65.2 (*a*)

Calculation based on inferred XRD values:

Based on the inferred XRD values, we can calculate (e.g. for the highest found Mn_{inc} in SRFA-containing samples, No. 8):

- Mn/Cd in the CdS solid = 0.27 / (1 - 0.27) = 0.33
- with Cd_{tot_ini} (Cd concentration at the beginning of the experiment) = 0.5 mmol L^{-1} (assuming all Cd was precipitated as CdS, as predicted by thermodynamic calculations):

➔ **Mn_{inc}** = 0.5 mmol L^{-1} x 0.33 = **0.167 mmol L^{-1}**

- Since Mn_{tot_ini} = 5 mmol L^{-1}: 5 - 0.167 = **4.833 mmol L^{-1} Mn** remain, that could be **adsorbed, flocculated with SRFA** or **freely dissolved in suspension**.

This shows, even based on the highest value found for Mn_{inc} (27.1 %), that a large fraction of Mn was either adsorbed to the CdS surface, flocculated with SRFA or freely dissolved in suspension.

Calculation based on total digests of the solids:

According to the digests of the SRFA-containing samples, Mn/Cd were between 0.7 (after 1 week) and 0.6 (after 8 weeks). Taking the average of these values, we can determine the average molar amount of **Mn in all potential solid phases** (also investigated with XAS):

- For average Mn/Cd = 0.65 and Cd_{tot_ini} = 0.5 mmol L^{-1}:

  0.65 x 0.5 mmol L^{-1} = **0.325 mmol L^{-1} Mn**

Compared with the values inferred from XRD calculations, about one third of the Mn in the solid phase was actually incorporated within sulfides, while the remaining major fraction in the solid phase was adsorbed or flocculated as Mn-SRFA. This matches well with the finding of the disappearing 2nd shell in the Mn *K*-edge Fourier transform data in all SRFA-containing samples.

Further, we can calculate that in accordance with the digest, about 5 – 0.325 = 4.675 mmol L^{-1} Mn (of the initial 5 mmol L^{-1} Mn) were in solution. Respecting that 50 mg C L^{-1} SRFA are equal to about 100 mg SRFA L^{-1} and that SRFA possesses a maximum binding capacity of roughly a bit less than 10 mmol g^{-1}, shows that the total binding capacity of the SRFA in our suspensions was about 1 mmol sites L^{-1}, which was considerably smaller than Mn in solution. Consequently, at higher Mn concentrations in solution (e.g. 5 mmol L^{-1}), it is expected that a large part of the SRFA is flocculated by Mn. At maximum, SRFA could precipitate 0.5 mmol L^{-1} Mn or rather a bit less, since not all SRFA sites are deprotonated.

Hence, the coagulated organics might contain about 10 % of the total Mn at maximum. At the same time, about 20 % (27.1 % at maximum) of Cd might be substituted by Mn, which corresponds to about 0.1 x 0.2 = 0.02 = 2 % of total Mn (factor 0.1 because total Mn was 10 times total Cd).

In summary, these calculations suggest that a large part of Mn in the SRFA-containing XAS samples (Fig. 6) was present as flocculated / precipitated Mn-SRFA and even dominated the spectra (10 % coagulated Mn-SRFA vs. 2 % Mn incorporated in the CdS structure). Since such a second co-precipitated phase besides the CdS would have also been spun down via centrifugation as well as retained by filters in the preparation of the XAS pellets, both phases were ultimately 'visible' in the XAS Mn *K*-edge spectra.

12. Cd *K*-edge EXAFS spectra and Fourier-transform magnitudes of CdS(-Mn) suspensions

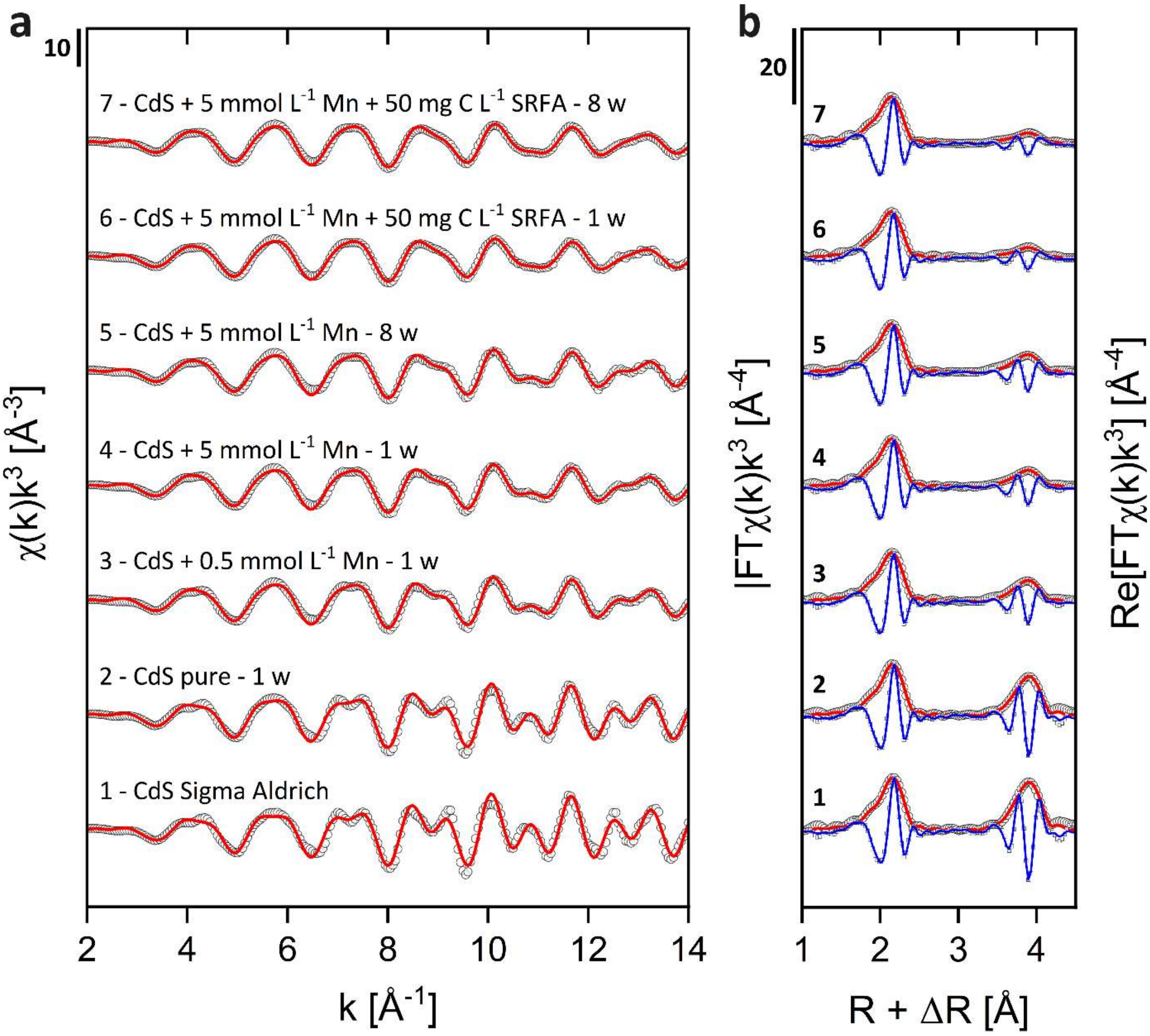

Figure S8: Cd *K*-edge EXAFS (a) spectra and Fourier-transform magnitudes (b) of concentrated colloidal CdS suspensions (500 µmol L^{-1} Cd(II) and 1000 µmol L^{-1} S(-II)) formed in the absence and presence of Mn^{2+} (0.5 and 5 mmol L^{-1}) and SRFA (50 mg C L^{-1}) at pH 7.5 in 10 mmol L^{-1} NaCl electrolyte after different aging times compared to the spectra of a crystalline CdS Sigma Aldrich reference. In (a and b) open circles represent experimental data and red lines designate the respective model fits. This figure shows the same data as Fig. 5 with added real parts (b, blue lines) enveloped by the Fourier-transform magnitudes.

13. Alternative shell fit for CdS reference

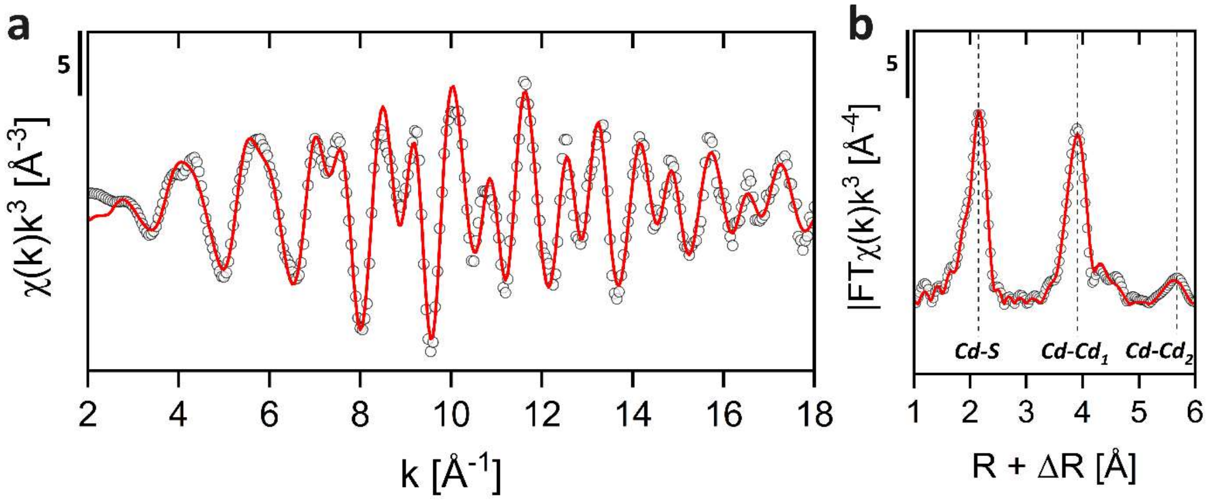

Figure S9: Cd *K*-edge EXAFS (a) spectra and Fourier-transform magnitudes (b) of the crystalline CdS Sigma Aldrich reference and corresponding alternative model fits using 4 single and 2 multiple scattering paths (cf. Tab. S6). In (a and b) open circles represent experimental data and red lines designate the respective model fits. For the alternative fits, path degeneracy for all paths was fixed (cf. Tab. S6).

Table S6: EXAFS parameters determined by shell fitting of the Cd *K*-edge EXAFS spectra of the crystalline CdS Sigma Aldrich reference using an alternative model that included 4 single and 2 multiple scattering paths.

No.	**Reference**	**SRFA (mg C L^{-1})**	**Mn^{2+} (mmol L^{-1})**	**Path**	**σ^2 (Å^2)**	**CN**	**R (Å)**	**ΔE_0 (eV)**	**R factor**	**Red χ^2**
1	Sigma Aldrich	0	0	Cd–S$_1$	0.003	4	2.530	9.6	0.027	445
				Cd–Cd$_1$	0.006	12	4.131			
				Cd–S$_1$-S$_1$	0.006	12	4.596			
				Cd–S$_1$-Cd$_1$	0.006	24	4.596			
				Cd–S$_2$	0.008	12	4.845			
				Cd–Cd$_2$	0.006	6	5.843			

14.TEM images of CdS in the presence of Mn and SRFA

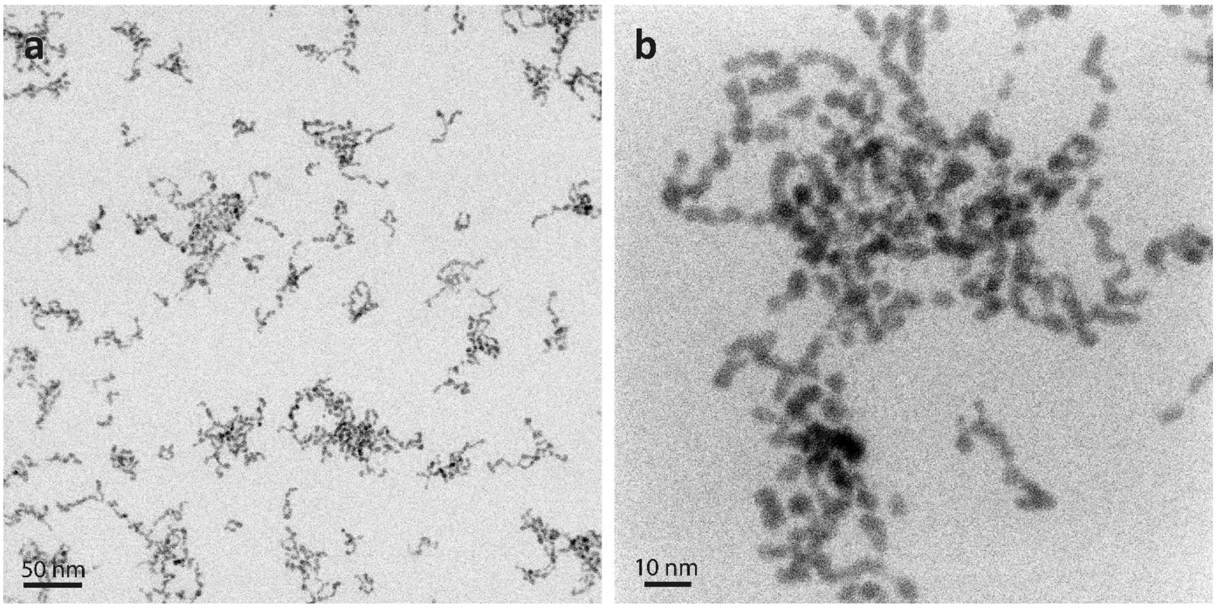

Figure S10: HAADF-TEM images (shown as inverted images) of a dilute CdS suspension (50 µmol L^{-1} Cd(II) and 100 µmol L^{-1} S(-II)) formed in the presence of 100 µmol L^{-1} Mn^{2+} and 50 mg C L^{-1} SRFA.

15. Mn *K*-edge EXAFS spectra and Fourier-transform magnitudes of CdS(-Mn) suspensions

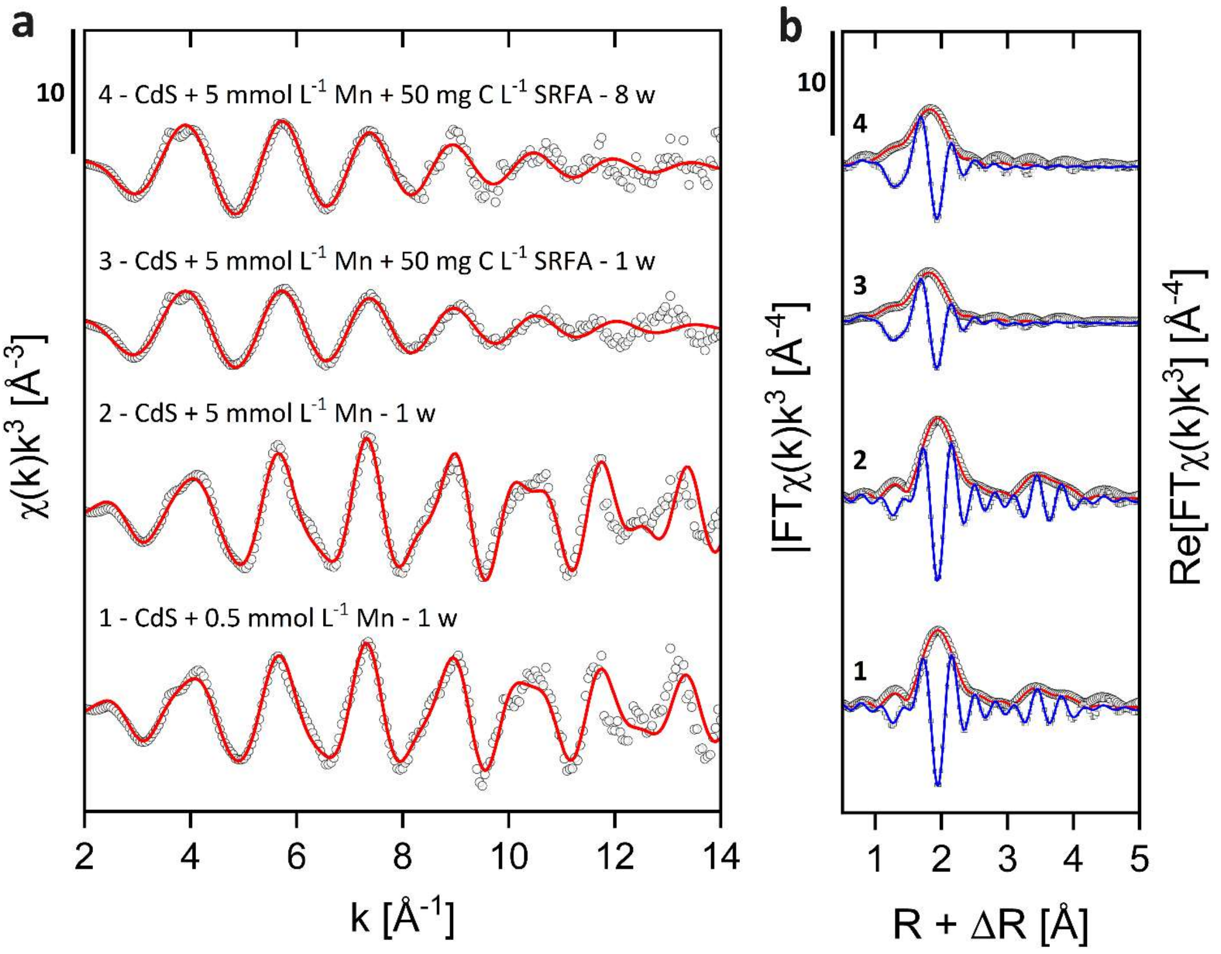

Figure S11: Mn *K*-edge EXAFS (a) spectra and Fourier-transform magnitudes (b) of concentrated colloidal CdS suspensions (500 µmol L^{-1} Cd(II) and 1000 µmol L^{-1} S(-II)) containing Mn^{2+} (0.5 and 5 mmol L^{-1}) and formed in the absence and presence of SRFA (50 mg C L^{-1}) at pH 7.5 in 10 mmol L^{-1} NaCl electrolyte after different aging times. In (a and b) open circles represent experimental data and red lines designate the respective model fits. This figure shows the same data as Fig. 6 with added real parts (b, blue lines) enveloped by the Fourier-transform magnitudes.

16. Alternative Mn *K*-edge Fourier-transform magnitudes of CdS(-Mn) suspensions in the presence of SRFA

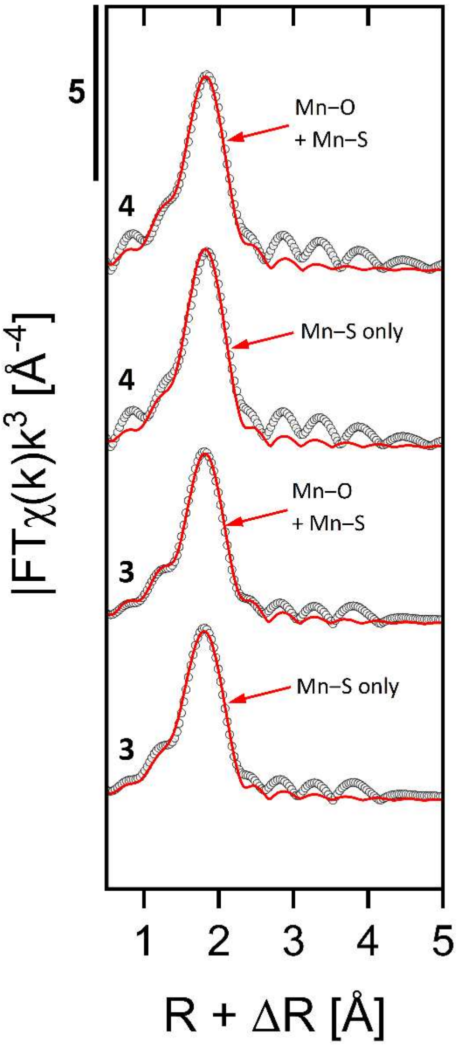

Figure S12: Fourier-transform magnitudes of Mn *K*-edge EXAFS spectra of concentrated colloidal CdS suspensions (500 µmol L^{-1} Cd(II) and 1000 µmol L^{-1} S(-II)) formed in the presence of 5 mmol L^{-1} Mn^{2+} and 50 mg C L^{-1} SRFA at pH 7.5 in 10 mmol L^{-1} NaCl electrolyte after 1 week (label '3') and 8 weeks (label '4') of aging. They constitute the same samples as shown in Fig. S11 labelled '3' and '4'. Open circles represent experimental data and red lines designate the respective model fits. First shell of sample spectra shown first for each sample were fitted with a Mn–S scattering path only, those directly above included a Mn–O and a Mn–S scattering path. Note that fitting was restricted between $R + \Delta R = 1.0 – 2.7$.

Table S7: EXAFS parameters determined by shell fitting of the Mn *K*-edge EXAFS spectra of concentrated colloidal CdS suspensions (500 µmol L^{-1} Cd(II) and 1000 µmol L^{-1} S(-II)) formed in the presence of 5 mmol L^{-1} Mn^{2+} and 50 mg C L^{-1} SRFA at pH 7.5 in 10 mmol L^{-1} NaCl electrolyte after different times of aging. EXAFS parameters are shown for shell fits only including one Mn–S single scattering path (cf. Fig. S12).

No.	**Aging time**	**SRFA (mg C L^{-1})**	**Mn^{2+} (mmol L^{-1})**	**Path**	**σ^2 (Å^2)**	**CN**	**R (Å)**	**ΔE_0 (eV)**	**R factor**	**Redχ^2**
3	1 w	50	5	Mn–S	0.013	6.18 ± 0.24	2.369	-9.9	0.011	541
4	8 w	50	5	Mn–S	0.001	6.19 ± 0.25	2.373	-9.3	0.012	310

17. Thermodynamic modeling of CdS suspensions in the presence of Mn(II) before and after sulfide addition

Table S8: Speciation of CdS suspensions *before* sulfide addition in the presence of Mn^{2+} as calculated with Visual MINTEQ 3.1. Suspensions with different Mn^{2+} and SRFA concentrations are presented (a-d).

a) 500 µmol L^{-1} Cd (II), 0 µmol L^{-1} S(-II), 500 µmol L^{-1} Mn(II), 0 mg C L^{-1} SRFA

Input

Species	Na^+ (mol L^{-1})	Cl^- (mol L^{-1})	MOPS (mol L^{-1})	SRFA (mg C L^{-1})	Cd(II) (µmol L^{-1})	Mn(II) (µmol L^{-1})	pH
Concentration	0.01	0.01	0.01	0	500	500	7.5

Distribution of components between dissolved and precipitated species (in mol L^{-1})

Component	Total dissolved	% dissolved	Total precipitated	% precipitated
Cd(II)	5.00E-04	100.00	0	0
Mn(II)	5.00E-04	100.00	0	0
Cl^-	1.00E-02	100.00	0	0

Dissolved data

Component	% of total concentration	Species
Cd^{2+}	61.0	Cd+2
	1.2	CdCl2(aq)
	0.1	CdOH+
	37.6	CdCl+
Mn^{2+}	99.3	Mn+2
	0.6	MnCl+
	0.1	MnOH+

Solids data

Mineral	Saturation index (= log IAP – log Ks)	Minerals precipitated	Equilibrium amount (mol L^{-1})
CdOHCl(s)	-1.788	none	0
$Cd(OH)_2$(s)	-2.339		
$CdCl_2$(s)	-7.147		
Pyrochroite ($Mn(OH)_2$)	-3.678		
Manganite (γ-MnO(OH))	-8.014		
Hausmannite ($Mn^{2+}Mn^{3+}{}_2O_4$)	-14.862		
Pyrolusite (β-MnO_2)	-18.245		

b) 500 µmol L^{-1} Cd (II), 0 µmol L^{-1} S(-II), 5000 µmol L^{-1} Mn(II), 0 mg C L^{-1} SRFA

Input

Species	Na^+ (mol L^{-1})	Cl^- (mol L^{-1})	MOPS (mol L^{-1})	SRFA (mg C L^{-1})	Cd(II) (µmol L^{-1})	Mn(II) (µmol L^{-1})	pH
Concentration	0.01	0.01	0.01	0	500	5000	7.5

Distribution of components between dissolved and precipitated species (in mol L^{-1})

Component	Total dissolved	% dissolved	Total precipitated	% precipitated
Cd(II)	5.00E-04	100.00	0	0
Mn(II)	5.00E-03	100.00	0	0
Cl^-	1.00E-02	100.00	0	0

Dissolved data

Component	% of total concentration	Species
Cd^{2+}	61.1	Cd+2
	1.2	CdCl2(aq)
	0.1	CdOH+
	37.5	CdCl+
Mn^{2+}	99.3	Mn+2
	0.6	MnCl+
	0.1	MnOH+

Solids data

Mineral	Saturation index (= log IAP – log Ks)	Minerals precipitated	Equilibrium amount (mol L^{-1})
CdOHCl(s)	-1.788	none	0
$Cd(OH)_2(s)$	-2.339		
$CdCl_2(s)$	-7.147		
Pyrochroite ($Mn(OH)_2$)	-2.678		
Manganite (γ-MnO(OH))	-7.014		
Hausmannite ($Mn^{2+}Mn^{3+}{}_2O_4$)	-11.862		
Pyrolusite (β-MnO_2)	-17.245		

c) 500 µmol L^{-1} Cd (II), 0 µmol L^{-1} S(-II), 500 µmol L^{-1} Mn(II), 50 mg C L^{-1} SRFA

Input

Species	Na^+ (mol L^{-1})	Cl^- (mol L^{-1})	MOPS (mol L^{-1})	SRFA (mg C L^{-1})	Cd(II) (µmol L^{-1})	Mn(II) (µmol L^{-1})	pH
Concentration	0.01	0.01	0.01	50	500	500	7.5

Distribution of components between dissolved and precipitated species (in mol L^{-1})

Component	**Total dissolved**	**% dissolved**	**Dissolved inorganic**	**Bound to DOM**	**% bound to DOM**	**Total precipitated**	**% precipitated**
Cd(II)	5.00E-04	100.00	3.97E-04	1.03E-04	20.6	0	0
Mn(II)	5.00E-04	100.00	4.00E-04	1.00E-04	20.0	0	0
Cl^-	1.00E-02	100.00	1.00E-02	0	0	0	0

Dissolved data

Component	**% of total concentration**	**Species**
Cd^{2+}	48.4	Cd+2
	0.3	(6)CdCl+D(aq)
	0.1	CdOH+
	29.9	CdCl+
	1.0	CdCl2(aq)
	8.8	(6)Cd+2D(aq)
	11.4	FA1-Cd(6)(aq)
	0.1	FA2-Cd(6)(aq)
Mn^{2+}	79.5	Mn2+
	0.05	MnOH+
	0.05	MnCl+
	14.4	(6)Mn+2D(aq)
	5.5	FA1-Mn(6)(aq)
	0.03	FA2-Mn(6)(aq)
HFA1-(6)(aq)	81.8	HFA1-(6)(aq)
	0.8	FA1-H(6)(aq)
	11.8	FA1-Cd(6)(aq)
	5.7	FA1-Mn(6)(aq)
HFA2-(6)(aq)	4.9	HFA2-(6)(aq)
	94.5	FA2-H(6)(aq)
	0.5	FA2-Cd(6)(aq)
	0.1	FA2-Mn(6)(aq)

Solids data

Mineral	Saturation index (= log IAP – log Ks)	Minerals precipitated	Equilibrium amount (mol L^{-1})
CdOHCl(s)	-1.887	none	0
$Cd(OH)_2$(s)	-2.440		
$CdCl_2$(s)	-7.245		
Pyrochroite ($Mn(OH)_2$)	-3.774		
Manganite (γ-MnO(OH))	-8.111		
Hausmannite ($Mn^{2+}Mn^{3+}{}_2O_4$)	-15.152		
Pyrolusite (β-MnO_2)	-18.341		

d) 500 µmol L^{-1} Cd (II), 0 µmol L^{-1} S(-II), 5000 µmol L^{-1} Mn(II), 50 mg C L^{-1} SRFA

Input

Species	Na^+ (mol L^{-1})	Cl^- (mol L^{-1})	MOPS (mol L^{-1})	SRFA (mg C L^{-1})	Cd(II) (µmol L^{-1})	Mn(II) (µmol L^{-1})	pH
Concentration	0.01	0.01	0.01	50	500	5000	7.5

Distribution of components between dissolved and precipitated species (in mol L^{-1})

Component	**Total dissolved**	**% dissolved**	**Dissolved inorganic**	**Bound to DOM**	**% bound to DOM**	**Total precipitated**	**% precipitated**
Cd(II)	5.00E-04	100.00	4.68E-04	3.20E-05	6.4	0	0
Mn(II)	5.00E-03	100.00	4.80E-03	2.00E-04	4.0	0	0
Cl^-	1.00E-02	100.00	1.00E-02	0	0	0	0

Dissolved data

Component	**% of total concentration**	**Species**
Cd^{2+}	57.2	Cd+2
	0.1	(6)CdCl+D(aq)
	0.1	CdOH+
	35.2	CdCl+
	1.2	CdCl2(aq)
	1.7	(6)Cd+2D(aq)
	4.4	FA1-Cd(6)(aq)
	0.1	FA2-Cd(6)(aq)
Mn^{2+}	95.3	Mn2+
	0.05	MnOH+
	0.6	MnCl+
	2.9	(6)Mn+2D(aq)
	1.1	FA1-Mn(6)(aq)
HFA1-(6)(aq)	84.0	HFA1-(6)(aq)
	0.4	FA1-H(6)(aq)
	4.6	FA1-Cd(6)(aq)
	11.0	FA1-Mn(6)(aq)
HFA2-(6)(aq)	7.6	HFA2-(6)(aq)
	91.8	FA2-H(6)(aq)
	0.4	FA2-Cd(6)(aq)
	0.2	FA2-Mn(6)(aq)

Solids data

Mineral	Saturation index (= log IAP – log Ks)	Minerals precipitated	Equilibrium amount (mol L^{-1})
CdOHCl(s)	-1.817	none	0
$Cd(OH)_2(s)$	-2.268		
$CdCl_2(s)$	-7.177		
Pyrochroite ($Mn(OH)_2$)	-2.695		
Manganite (γ-MnO(OH))	-7.032		
Hausmannite ($Mn^{2+}Mn^{3+}{}_2O_4$)	-11.915		
Pyrolusite (β-MnO_2)	-17.262		

Table S9: Speciation of CdS suspensions *after* sulfide addition in the presence of Mn^{2+} as calculated with Visual MINTEQ 3.1. Suspensions with different Mn^{2+} and SRFA concentrations are presented (a-d).

---

a) 500 µmol L^{-1} Cd (II), 1000 µmol L^{-1} S(-II), 500 µmol L^{-1} Mn(II), 0 mg C L^{-1} SRFA

Input

at pH 7.5

Species	Na^+ (mol L^{-1})	Cl^- (mol L^{-1})	MOPS (mol L^{-1})	SRFA (mg C L^{-1})	Cd(II) (µmol L^{-1})	Mn(II) (µmol L^{-1})	S(-II) (µmol L^{-1})
Concentration	0.01	0.01	0.01	0	500	500	1000

Distribution of components between dissolved and precipitated species (in mol L^{-1})

Component	Total dissolved	% dissolved	Total precipitated	% precipitated
Cd(II)	0	0	5.00E-04	100.00
Mn(II)	5.00E-04	100.00	0	0
HS^-	2.67E-05	2.67	9.73E-04	97.33

Dissolved data (Mn^{2+} and HS^- only)

Component	% of total concentration	Species
Mn^{2+}	94.1	Mn2+
	0.05	MnOH+
	0.6	MnCl+
	5.2	MnHS+
HS^-	2.3	HS-1
	0.7	H2S(aq)
	97.1	MnHS+

Solids data

Mineral	Saturation index (= log IAP – log Ks)	Minerals precipitated	Equilibrium amount (mol L^{-1})
Greenockite	0	Greenockite	5.00E-04
Sulfur(s)	0	Sulfur(s)	4.73E-04
CdOHCl(s)	-13.34		
$Cd(OH)_2$(s)	-13.90		
$CdCl_2$(s)	-18.69		
MnS (green)	-2.251		
MnS (pink)	-5.251		
Pyrochroite ($Mn(OH)_2$)	-3.701		
Manganite (γ-MnO(OH))	-8.038		
Hausmannite ($Mn^{2+}Mn^{3+}{}_2O_4$)	-14.933		
Pyrolusite (β-MnO_2)	-18.268		

b) 500 µmol L^{-1} Cd (II), 1000 µmol L^{-1} S(-II), 5000 µmol L^{-1} Mn(II), 0 mg C L^{-1} SRFA

Input

at pH 7.5

Species	Na^+ (mol L^{-1})	Cl^- (mol L^{-1})	MOPS (mol L^{-1})	SRFA (mg C L^{-1})	Cd(II) (µmol L^{-1})	Mn(II) (µmol L^{-1})	S(-II) (µmol L^{-1})
Concentration	0.01	0.01	0.01	0	500	5000	1000

Distribution of components between dissolved and precipitated species (in mol L^{-1})

Component	Total dissolved	% dissolved	Total precipitated	% precipitated
Cd(II)	0	0	5.00E-04	100.00
Mn(II)	5.00E-03	100.00	0	0
HS^-	2.60E-04	26.00	7.40E-04	74.00

Dissolved data (Mn^{2+} and HS^- only)

Component	% of total concentration	Species
Mn^{2+}	94.1	Mn2+
	0.05	MnOH+
	0.6	MnCl+
	5.2	MnHS+
HS^-	0.2	HS-1
	0.1	H2S(aq)
	99.7	MnHS+

Solids data

Mineral	Saturation index (= log IAP – log Ks)	Minerals precipitated	Equilibrium amount (mol L^{-1})
Greenockite	0	Greenockite	5.00E-04
Sulfur(s)	0	Sulfur(s)	2.40E-04
CdOHCl(s)	-13.34		
$Cd(OH)_2$(s)	-13.90		
$CdCl_2$(s)	-18.69		
MnS (green)	-1.251		
MnS (pink)	-4.251		
Pyrochroite ($Mn(OH)_2$)	-2.702		
Manganite (γ-MnO(OH))	-7.038		
Hausmannite ($Mn^{2+}Mn^{3+}{}_2O_4$)	-11.933		
Pyrolusite (β-MnO_2)	-17.268		

c) 500 µmol L^{-1} Cd (II), 1000 µmol L^{-1} S(-II), 500 µmol L^{-1} Mn(II), 50 mg C L^{-1} SRFA

Input

at pH 7.5

Species	Na^+ (mol L^{-1})	Cl^- (mol L^{-1})	MOPS (mol L^{-1})	SRFA (mg C L^{-1})	Cd(II) (µmol L^{-1})	Mn(II) (µmol L^{-1})	S(-II) (µmol L^{-1})
Concentration	0.01	0.01	0.01	50	500	500	1000

Distribution of components between dissolved and precipitated species (in mol L^{-1})

Component	**Total dissolved**	**% dissolved**	**Dissolved inorganic**	**Bound to DOM**	**% bound to DOM**	**Total precipitated**	**% precipitated**
Cd(II)	0	0	0	0	0	5.00E-04	100.00
Mn(II)	5.00E-04	100.00	3.22E-04	1.78E-04	35.6	0	0
HS^-	1.74E-05	1.75	1.74E-05	0	0	9.83E-04	98.25

Dissolved data (Mn^{2+}, HS^- and SRFA only)

Component	**% of total concentration**	**Species**
Mn^{2+}	60.6	Mn2+
	0.05	MnOH+
	0.4	MnCl+
	3.3	MnHS+
	24.2	(6)Mn+2D(aq)
	11.4	FA1-Mn(6)(aq)
	0.03	FA2-Mn(6)(aq)
HS^-	3.5	HS-1
	1.0	H2S(aq)
	95.5	MnHS+
HFA1-(6)(aq)	86.8	HFA1-(6)(aq)
	1.4	FA1-H(6)(aq)
	11.8	FA1-Mn(6)(aq)
HFA2-(6)(aq)	3.8	HFA2-(6)(aq)
	96.1	FA2-H(6)(aq)
	0.1	FA2-Mn(6)(aq)

Solids data

Mineral	**Saturation index (= log IAP – log Ks)**	**Minerals precipitated**	**Equilibrium amount (mol L^{-1})**
Greenockite	0	Greenockite	5.00E-04
Sulfur(s)	0	Sulfur(s)	4.83E-04
CdOHCl(s)	-13.34		

$Cd(OH)_2(s)$	-13.90		
$CdCl_2(s)$	-18.69		
MnS (green)	-2.442		
MnS (pink)	-5.442		
Pyrochroite ($Mn(OH)_2$)	-3.893		
Manganite (γ-MnO(OH))	-8.229		
Hausmannite ($Mn^{2+}Mn^{3+}{}_2O_4$)	-15.507		
Pyrolusite (β-MnO_2)	-18.460		

d) 500 µmol L^{-1} Cd (II), 1000 µmol L^{-1} S(-II), 5000 µmol L^{-1} Mn(II), 50 mg C L^{-1} SRFA

Input at pH 7.5

Species	Na^+ (mol L^{-1})	Cl^- (mol L^{-1})	MOPS (mol L^{-1})	SRFA (mg C L^{-1})	Cd(II) (µmol L^{-1})	Mn(II) (µmol L^{-1})	S(-II) (µmol L^{-1})
Concentration	0.01	0.01	0.01	50	500	5000	1000

Distribution of components between dissolved and precipitated species (in mol L^{-1})

Component	Total dissolved	% dissolved	Dissolved inorganic	Bound to DOM	% bound to DOM	Total precipitated	% precipitated
Cd(II)	0	0	0	0	0	5.00E-04	100.00
Mn(II)	5.00E-03	100.00	4.77E-04	2.28E-04	4.6	0	0
HS^-	2.48E-04	24.83	2.48E-04	0	0	7.52E-04	75.17

Dissolved data (Mn^{2+}, HS^- and SRFA only)

Component	% of total concentration	Species
Mn^{2+}	89.8	Mn2+
	0.05	MnOH+
	0.6	MnCl+
	5.0	MnHS+
	3.2	(6)Mn+2D(aq)
	1.3	FA1-Mn(6)(aq)
HS^-	0.2	HS-1
	0.1	H2S(aq)
	99.7	MnHS+
HFA1-(6)(aq)	85.8	HFA1-(6)(aq)
	0.6	FA1-H(6)(aq)
	13.6	FA1-Mn(6)(aq)
HFA2-(6)(aq)	7.1	HFA2-(6)(aq)
	92.7	FA2-H(6)(aq)
	0.2	FA2-Mn(6)(aq)

Solids data

Mineral	Saturation index (= log IAP – log Ks)	Minerals precipitated	Equilibrium amount (mol L^{-1})
Greenockite	0	Greenockite	5.00E-04
Sulfur(s)	0	Sulfur(s)	2.52E-04
CdOHCl(s)	-13.34		

$Cd(OH)_2(s)$	-13.90		
$CdCl_2(s)$	-18.69		
MnS (green)	-1.271		
MnS (pink)	-4.271		
Pyrochroite ($Mn(OH)_2$)	-2.722		
Manganite (γ-$MnO(OH)$)	-7.058		
Hausmannite ($Mn^{2+}Mn^{3+}{}_2O_4$)	-11.994		
Pyrolusite (β-MnO_2)	-17.289		

References

1. Gustafsson, J. P., Visual MINTEQ ver. 3.1, 2013.
2. Milne, C. J., Kinniburgh, D. G., van Riemsdijk, W. H. and Tipping, E., Generic NICA−Donnan model parameters for metal-ion binding by humic substances, *Environ. Sci. Technol.*, 2003, **37**, 958-971.
3. Rodic, D., Spasojevic, V., Bajorek, A. and Onnerud, P., Similarity of structure properties of Hg1−xMnxS and Cd1−xMnxS (structure properties of HgMnS and CdMnS), *J. Magnetism Magnetic Materials*, 1996, **152**, 159-164.